The Molecular Basis for Properties of Binary Solvent Systems: Synchrotron X-ray Pair Distribution Function Analysis of the Acetone-Water System

Anuradha R. Pallipurath1,2, Bethan Evans1, Arturs Pugejs1, Philip A. Chater3 and Sven L. M. Schroeder1-3**

1. School of Chemical and Process Engineering, University of Leeds, Leeds LS2 9JT, UK.

2. Research Complex at Harwell, Didcot, Oxfordshire, OX11 0DE, UK

3. Diamond Light Source Ltd., Didcot, Oxfordshire, OX11 0DE, UK

Corresponding Author

*corresponding author: s.l.m.schroeder@leeds.ac.uk; a.r.pallipurath@leeds.ac.uk

ABSTRACT The acetone-water phase diagram. Dynamic structural insights into intermolecular interactions in acetone-water binary mixtures modelled from synchrotron total X-ray scattering describes phase behavior.

TOC GRAPHICS

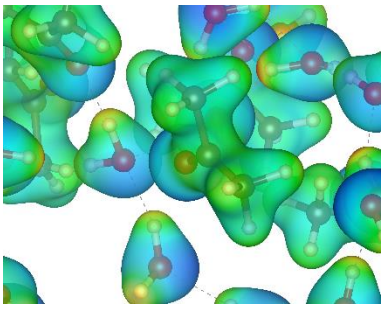

KEYWORDS Water-acetone binaries, X-ray pair distribution functions, EPSR, electrostatic potentials, Phase behaviour

Through the use of solvent mixtures one can create liquid solution media with tailored physicochemical properties, for example, solubility, viscosity, vapour pressure, dielectric constant or polarity. In principle, solvent combination creates an immense design space for practical applications such as chemical synthesis, separation processes, product formulation and functional fluidics. Binary and ternary mixtures of solvents are widely used to obtain optimal properties in separations, with extractive distillation[1] and crystallisation[2] among the better known examples. Use of a solvent mixtures is believed to create a preferential solvation scenarios,[3–5] in which solubility is regulated by preferential molecular association of a solute with one solvent component, which may then facilitate a synergistic effect with the other solvent component, for example by enhancing solubility by modifying the balance between hydrophilic and hydrophobic interactions. For organic solutes, computational studies have indicated that preferential solvation in binary solvent mixtures can be a strategy for achieving polymorph control.[6]

Molecular dynamics methods are widely used to predict the molecular structure of solvent and solution mixtures. Methods such as Kirkwood-Buff analysis can then be used to calculate thermodynamic properties from the pair correlations in the predicted structures.[7,8] Such statistical mechanics analyses are valuable, as even when they do not predict macroscopic observables quantitatively they can stimulate deeper thinking about the impact of local molecular interactions on solvent behaviour.

Among the most powerful experimental techniques for probing the local molecular structure in liquids (and thus validating molecular dynamics predictions) has been neutron pair distribution function analysis (NPDF).[9–11] When used in combination with Empirical Potential Structure Refinement (EPSR) Monte-Carlo modelling,[12] neutron scattering data can be used to identify statistically significant structure models that allow relating local molecular interactions to solution

properties. EPSR of NPDF has previously been used to study solvent binaries[9,13] and ionic liquids.[14] An immense advantage of NPDF is the high cross section for neutron scattering from hydrogen atoms, whose precise location is often essential for understanding solution structure driven by non-covalent interactions such as hydrogen bonding. Especially when combined with NPDF of the corresponding deuterated systems and with laboratory based X-ray PDF measurements it provides precise insight into the local interactions in binary systems of one given concentration.[15] A drawback of this in-depth analysis is the need for access to a spallation neutron source and the isotopically tagged (usually deuterated) systems. More importantly, acquiring a complete set of such complementary experimental data represents at minimum one day of measurement work. These limitations may be too severe to allow advancing the molecular science of binary and, ultimately, multi-component solvent systems, which requires understanding of relationships between molecular structure and macroscopically observable properties across whole phase diagrams. In other words, PDF analysis at multiple composition points are realistically needed to obtain the molecular basis for phase behaviour as a function of system composition.

Here, we wish to demonstrate how synchrotron X-ray pair distribution function (XPDF) analysis[16] presents a compromise alternative to NPDF analysis. We will argue that the structure insight, while not as detailed (especially hydrogen positions cannot be determined), is sufficient to obtain an overview over structure variations associated with property trends and discontinuities in the phase diagram. Most importantly, synchrotron XPDF combines rapid data collection (on a scale of minutes per PDF) with simplified sample preparation (no deuteration) and use of straightforward scattering geometries.[17] Even though organic systems are characterised by relatively weak X-ray scattering cross sections, the data quality is sufficient that one can even envisage variable temperature and other in-situ studies. Our previous studies[15] and others in the

literature[18], have validated the structures obtained from XPDF against those modelled from NPDF, thereby overcoming the limitations of XPDF in getting information to a high Q value compared to NPDF.

We have chosen the acetone-water binary system for this demonstration study because there is already a wealth of information for comparison in the literature, including macroscopic observables such as vapour pressures[19–21], spectroscopic signatures[22–27], NPDF structures of pure acetone[28] and some aqueous mixtures[29], as well as a structure obtained using a Mo K_α laboratory diffractometer.[30]

Detailed information about experimental and structure modelling methods can be found in the supporting information. We will label samples according to the mol% composition, e.g. A90_W10 indicates 90 mol% acetone and 10 mol% water. The mixtures were prepared in borosilicate capillaries that were sealed by melting the glass to prevent any composition changes due to preferential evaporation of the more volatile component. Total X-ray scattering data were collected in 10 min per sample.

The post-processed F(Q) data were then used to refine structural models using Empirical Potential Structure Refinement (EPSR) software. Lennard-Jones potentials (details available in the supporting information) for different atom types described in **Chart 1**, were used to generate pair-wise potentials. Water molecules in the various systems were modelled as a 'two-potential' system with equal numbers of molecules with SPC/E and TIP3P potentials, due to growing evidence for the same[313233], and because it also proved to be better fits for our experimental data (Figure 1).

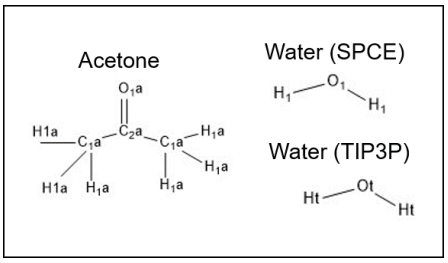

Chart 1: Lennard-Jones atom types used during the Empirical potential structure refinement.

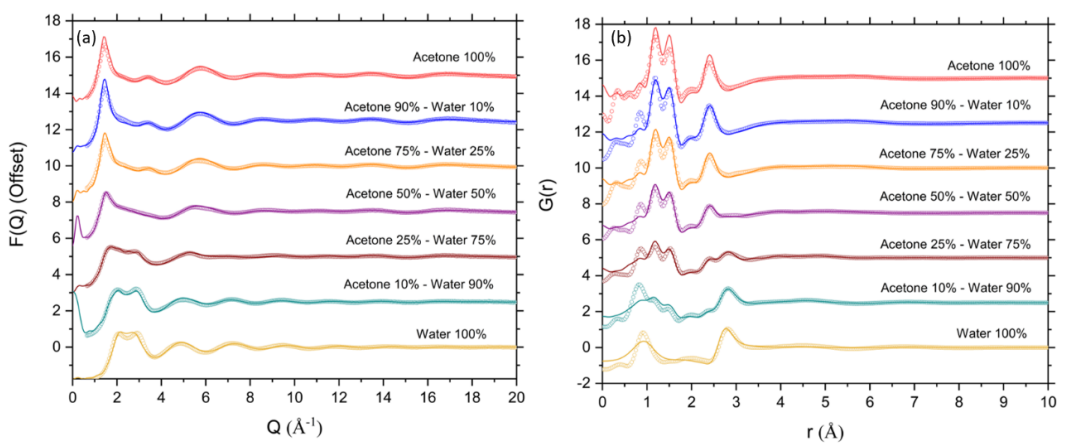

Figure 1: a) Total X-ray scattering data from a series of Acetone-water binaries as a function of composition; b) corresponding X-ray pair distribution functions. Experimental data are shown as dots, while solid lines are the fits to the data obtained by EPSR.

Thermodynamics of the mixtures: A10_W90 has the lowest reference potential (RP) energy, as well as the lowest average intermolecular energy (AIME) amongst all compositions (**Figure 2a**). Probabilities calculated from the partition functions generated during the structure optimisation (**Figure 2b**), shows both pure water and the A10_W90 composition have distinct local structures that have higher probability of contribution to the overall solution structure. This suggests a certain

rigidity in the local structure, which could result in increased inter-molecular interactions, evidenced also by the drastic decrease in the AIME. This behaviour explains the increase in kinematic viscosity of the A10_W90 system over and above that of pure water itself[34].

A25_W75 system in a high pressure state is predicted to be the most stable structure amongst all the binary compositions[21]. Thermodynamic mixing energies estimated from the Helmholtz energy (A), internal energy (U) and the temperature-dependant entropy (TS) of pure water and acetone, revealed that the A25_W75 composition in fact has the lowest mixing energy, thereby suggesting the adaptation of a more stable structure. It can also be noted that these contributions are purely enthalpic, with little contribution from the entropy of mixing unlike the study by Benedetti et. al., whose experiments weren't carried out at constant volume[20]. True thermodynamic values for each system can be found in the supporting information (Figure S2). A plot of the molar volume occupation of each molecular component in their simulation box, also suggests that, at the A25_W75 composition the molar volume occupation of both components are closest to being near equivalent (61.7% acetone and 45.1% water), with a 3.95% decrease in the expected total molar volume (**Figure S3**).

Most higher concentrations of acetone in the aqueous binaries, especially the 90A_W10 has been reported to generate higher solubilites of organics,[35,36] sometimes even compared to pure acetone itself. It can be seen from **Figure 2d** that pure acetone has the largest standard deviation in the change in average dipole moments in the system, while the addition of a small amount of water, decreases this variation drastically. Further addition of water leads to progressive increase in the variation of average dipole moments. The minimal fluctuation of dipole moments in 90A_W10 system, could provide for a more stable environment, without the presence of sudden changes in induced dipoles, thereby enabling the increase in solubilities of organics in this phase. The effect

of solvation shells around solutes in these systems are currently under investigation and are beyond the scope of the current study.

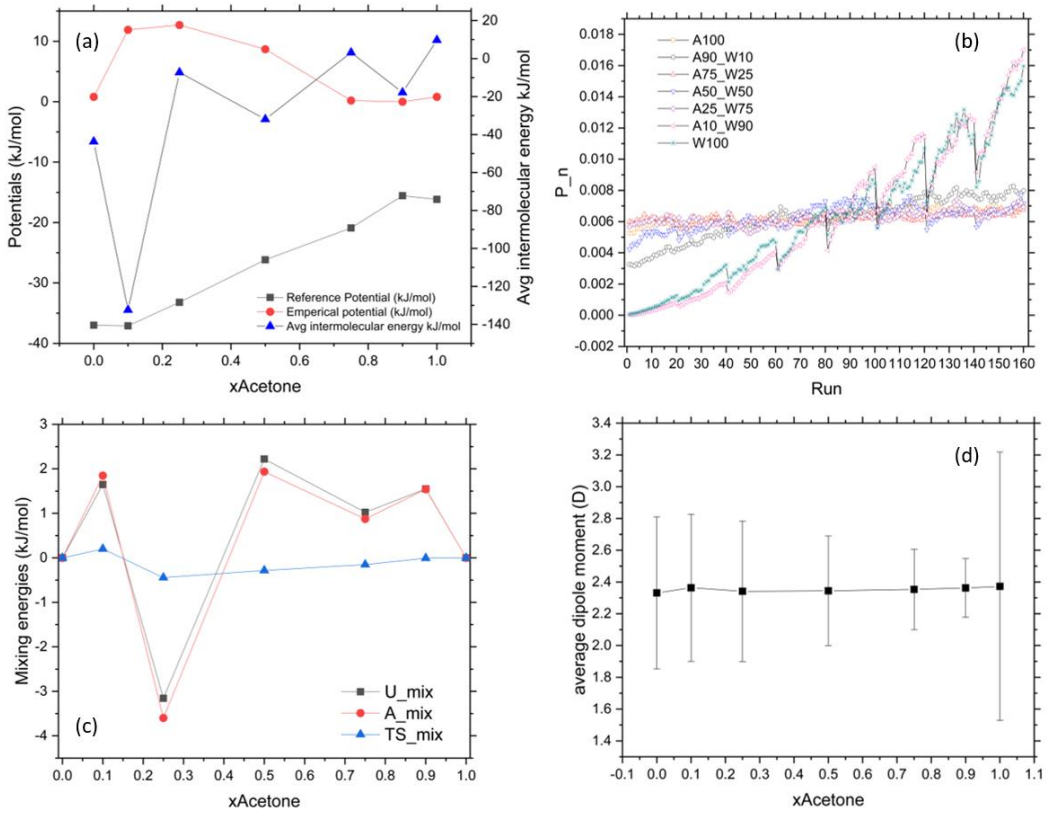

Figure 2: (a) Reference potential energy of a box of 1000 molecules, the allowed width of Empirical potential oscillations in a system and the average intermolecular energy (per molecule) of each composition, (b) Probability of occurrence of various configurations during the reference potential refinements derived from its partition functions; (c) Thermodynamics of mixing obtained from the Helmholtz energy, internal energy and entropy of pure water and acetone during reference potential refinements; (d) average dipole moments of a box of 1000 molecules obtained after reference and empirical potential refinements.

Pair distribution function analysis: The origin of the interesting phase behaviour and the related thermodynamics can be attributed to individual pair correlations, both self and hetero interactions. Assuming the carbonyl carbon of acetone (C2a) as the centre of mass, the partial pair correlations (g(r)) with surrounding acetone molecules (Figure 3a) reveal that the A10_W90 composition have closer self-interactions in the second (8.18Å compared to 9 Å in the rest) and third zones (indicated by *), compared to the other compositions and pure acetone itself. This composition also shows C2a-O1a self-interactions at a slightly longer distance compared to the rest (6.7Å compared to 6.1Å in the rest), as well as the presence of new interactions at 13.7Å (indicated by * in **Figure 3b**). Carbonyl C2a also develops interactions with oxygen in water at short distances of ~3.89 Å as predicted by unlike-induced interactions using the Mie-SAFT theory[37]. On the contrary, O-O correlations in water and the A10_W90 composition practically remains the same, while the secondary interactions occur at a longer distance and the tertiary interactions completely vanish beyond the 50-50 composition (**Figure 3c**), possibly owing to the relatively lesser number of water molecules leading to lesser number of said interactions. This also seems to directly relate the observed intensities as a result of the scattering power to the correlation, as previously discussed.[38]

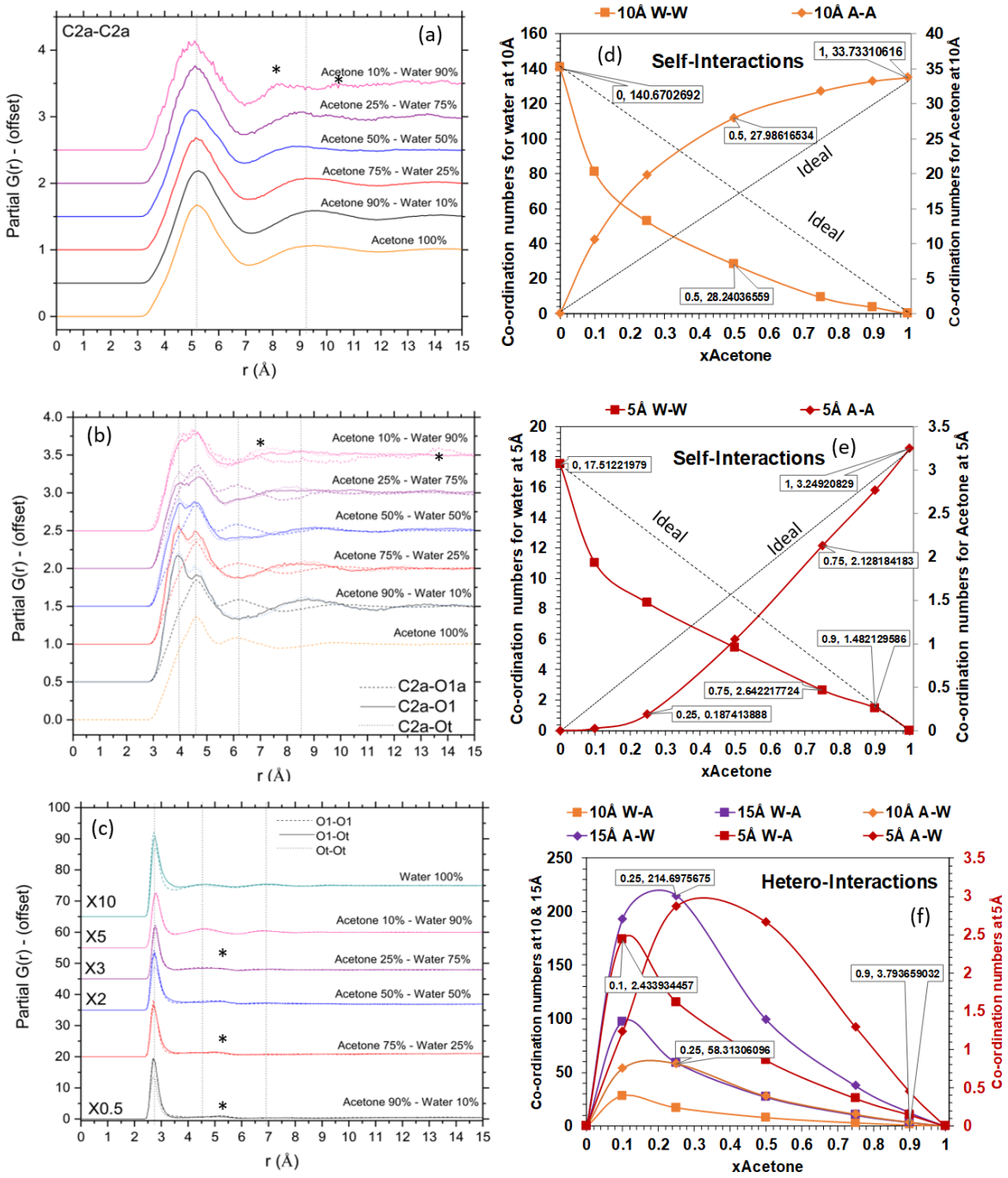

Figure 3: a) Partial pair correlation functions arising from the interactions between carbonyl carbons (C2a) of adjacent acetone molecules; b) Partial pair correlation functions arising from the interactions between carbonyl carbon (C2a) and oxygen in acetone (O2a), and of the water molecules represented by two potentials (O1 and Ot); (c) Partial pair correlation functions arising

from the interactions between oxygen atoms in water molecules represented by two potentials (O1 and Ot); * in the figures show significant differences in the pair correlations as compared to the pure solvent and dotted lines act as a guide to the eye to identify shifts in pair correlations with respect to that of the pure solvent; (d) Running co-ordination numbers at 10 Å, for self-interactions; (e) Running co-ordination numbers at 5 Å, for self-interactions; the dotted lines represent co-ordinations expected for an ideal behaviour; (f) Running co-ordination numbers at 5, 10 and 15 Å, for hetero-interactions.

Calculation of the running co-ordination numbers around both acetone and water in these systems gives a better insight into the self and hetero interactions that dominate phase behaviour. While the inter-molecular self-interactions of both components deviate from ideal behaviour, it is interesting to note the absence of any acetone-acetone interactions within 5 Å in the high water concentration compositions, and at higher acetone concentrations, a linear near-ideal behaviour is observed (**Figure 3e**). These observations are in line with the expected[39] dominance of hetero interactions in the system relative to the self-interactions. The acetone-water hydrogen bond appears to be the driving force for structure formation in the system, with no acetone-acetone self-interactions at acetone concentrations below 20mol%. In the case of water intermolecular self-interactions, an ideal behaviour is observed in the A90_W10 composition, with a sudden marked deviation from ideality with increasing amounts of water. Pure solvents have the highest number of self-interactions amongst all composition, with water having the expected 17.5 surrounding waters within 5 Å radius, and acetone having 3.2 other acetones around it, within a 5 Å radius, as opposed the expected 4.2 acetones based on its experimental densities. At 5 Å the 75A_25W composition has equal number of self-interactions in both components (~2.1- 2.4), while at 10 Å,

the 50A_50W composition has equal number of self-interactions (~28). As can be seen from **Figure 4f**, A25_W75 composition has the highest number of acetone-water (acetone central molecule) and water-acetone (water central molecule) hetero-interactions at all distances. Within 10 Å however, at the A90_W10 composition, 4 hetero-interactions with both acetone and water as the central molecule, suggests the presence of tetrahedral H-bonds between carbonyl O1a and water, which is similar to the water self-interactions in this system. This ideal interaction could be the reason for the formation of a low-boiling azeotrope at this composition.[37] At high acetone concentration spectroscopic studies also revealed an increase in the acetone-water hetero and water-water self-interaction lifetimes suggesting co-operative motion in the liquid.[22] Cumulative number of interactions (**Figure S3**) indicate that at longer distances beyond the first interaction shell, acetone in the A25_W75 composition has the highest number of nearest neighbour interactions, supporting the presence of the most stable structure. Within 5 Å, the 50A_50W composition has 3.7 nearest neighbour interactions, which is the highest amongst all compositions, including that of pure acetone. This stronger hetero-interactions than self-interactions in acetone was predicted from experimental thermodynamic experiments[20]. Cumulative co-ordination numbers around a central water molecule increases steadily with increase in water in the composition and is never as densely packed as pure water itself, at all length scales.

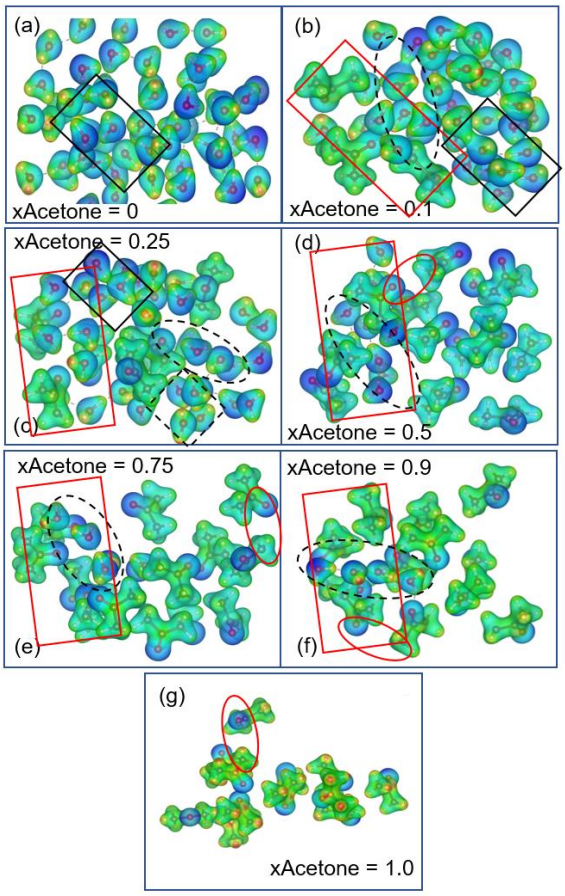

Figure 4: Electron density maps coloured using electrostatic potentials (red – electron deficient and blue – electron rich regions) for the acetone-water binary series. Red rectangular box highlights hydrated acetone molecules interacting with each other; black rectangular box highlights rigid tetrahedral H-bonding in water; dotted black rectangular box highlights four-membered rings of H-bonded water; black dotted ellipses highlight chains of H-bonded water molecules; red ellipses highlight H-bond-like electrostatic interactions between a carbonyl O in acetone (O1a) and an alkyl H in acetone (H1a).

Electrostatic potential calculation: To gain better insights into the nature of these molecular interactions, snapshots of the solution structures optimised against experimental data, were subject

to single point energy calculations using density functional theory, followed by the generation of the electron density maps and the electrostatic potentials (ESP). These maps show a clear picture of the location of the electron densities that influence most molecular interactions. **Figure 4** illustrates examples of these snapshots and highlights the various interactions observed. In higher concentrations of water including pure water itself, a central water molecule surrounded a tetrahedron of H-bonded water is a recurring feature (**Figure 4 a-c** indicated by a black box). Another common feature is the presence of a chain of H-bonded water molecules in all binary compositions (**Figure 4 b – f**, dotted ellipse), suggesting that the water molecules are more loosely bound in the presence of acetone, this was also evidenced in a recent Raman spectroscopic investigation of the systems[27] and the NPDF study which saw decrease in the water co-ordination with increasing acetone[29]. The presence of the tetrahedrally H-bonded water indicates a certain rigidity in the H-bonded network in pure water and also in the A10_W90 composition, as observed from the contributions of configurations to the partition functions in **Figure 2b**. These snapshots also reveal that individual acetone molecules are hydrated and the hydrated acetones interact with other such units. These molecular units are highlighted in a red box in **Figure 4**. This is also observed in the fact that features in g(r) corresponding to C2a-O1 and C2a-Ot occur at a short distance (~3.89 Å) compared to that of C2a-O1a intermolecular-interactions (~4.6 Å). These observations are similar to our findings in the solution structure of imidazole, where individual units are hydrated and the secondary interactions are between these hydrated units,[15] unlike the structure proposed by Max et. al using factor analysis of infrared spectroscopy.[24] Toryanik et.al. measured low self-diffusion in compositions between 15 -20 mol% acetone,[21] which agrees well with the reported increase in kinematic viscosities.[34] Molar volume is inversely proportional to observed self-diffusion[21]. Assuming these hydrated acetones act as a unit, the calculated molar

volume increase from that of a single acetone peaks at 25A_75W composition (**Figure S3**). Even though the %molar volume of these hydrated units are higher for higher acetone concentrations, the statistical probability of their occurrence is much lower compared to the 10A_90W and 25A_75W compositions, showing that the increased molar volume of these units lead to a decrease in the self-diffusion and hence increase in viscosities. Another recurring feature in the ESP maps of all the compositions, including that of pure acetone is the presence of intermolecular interactions between the carbonyl O1a and the alkyl H1a, as observed in the NPDF analysis[28]. A full structural analysis of all the features in these system will be published subsequently in a full article. The colour gradient in the ESP of pure acetone indicates the presence of strong dipoles within the molecules, compared to the acetones in the binary composition, supporting our earlier finding of large standard deviations in the average dipole moments in the simulation box of pure acetone.

In conclusion, we have used total X-ray scattering and pair distribution function analysis to develop structural models that provide direct insight into molecular origin of trends in the phase diagram. These provide a first molecular basis for understanding the deviations from ideal behaviour in acetone-water binary molar mixtures. In line with previous thermodynamic models, the acetone-water bonding is the dominant force that structures the solutions. As a result, interactions between hydrated acetone molecules are the most recurring structural feature. Our analysis indicates that 10% acetone in water has the highest kinematic viscosity due to the system having much lower average intermolecular energy, as well as higher contributions from rigid structural features that involve tetrahedrally H-bonded waters, and higher probability of hydrated acetone units occupying more molar volume, thereby decreasing self-diffusion in the system. Around 25% acetone in water has the most stable structure, as it is the composition that has near-equivalent molar volume contributions from both components and is the composition with the

highest nearest-neighbour interactions around a central acetone molecule. 90% acetone forms a low-boiling azeotrope, as it has near-ideal behaviour in intermolecular self-interactions in both components and has equal number of hetero-interactions around both components. It also has the highest ability to increase solubility of organics due to the lowest variation in average dipole moments, providing a more stable environment for a solute. Further investigations on the effect of this composition on solutes are underway.

ASSOCIATED CONTENT

The supporting information has detailed experimental and structure modelling methodologies employed, together with details of the thermodynamic calculations carried out subsequently.

AUTHOR INFORMATION

Notes

The authors declare no competing financial interests.

ACKNOWLEDGMENT

The authors wish to acknowledge the allocation of beamtime at Diamond Light Source . SLMS acknowledges the Royal Academy of Engineering, Diamond Light Source Ltd and Infineum UK for support of the Bragg Centenary Chair. SLMS and AP acknowledge the use of laboratory facilities at the Research Complex at Harwell, with financial support from the Future Continuous Manufacturing and Advanced Crystallisation (CMAC) Hub (EPSRC Grant EP/P006965/1). The authors thank Daniel Bowron and Jonathan Skelton for their advice. BE and AP wish to acknowledge the EPSRC CP3 CDT for funding their PhD studentships (EP/L015285/1).

REFERENCES

(1) Lei, Z. Azeotropic Distillation. *Ref. Modul. Chem. Mol. Sci. Chem. Eng.* **2017**, No. January, 0–8. https://doi.org/10.1016/b978-0-12-409547-2.06018-2.

(2) Belenguer, A. M.; Lampronti, G. I.; Cruz-Cabeza, A. J.; Hunter, C. A.; Sanders, J. K. M. Solvation and Surface Effects on Polymorph Stabilities at the Nanoscale. *Chem. Sci.* **2016**, *7* (11), 6617–6627. https://doi.org/10.1039/c6sc03457h.

(3) Papadakis, R.; Deligkiozi, I.; Nowak, K. E. Study of the Preferential Solvation Effects in Binary Solvent Mixtures with the Use of Intensely Solvatochromic Azobenzene Involving [2]Rotaxane Solutes. *J. Mol. Liq.* **2019**, *274*, 715–723. https://doi.org/10.1016/j.molliq.2018.10.164.

(4) Marcus, Y. Preferential Solvation in Mixed Solvents X. Completely Miscible Aqueous Co-Solvent Binary Mixtures at 298.15 K. *Monatshefte fur Chemie* **2001**, *132* (11), 1387–1411. https://doi.org/10.1007/s007060170023.

(5) Marcus, Y. Preferential Solvation in Binary Mixed Solvents. *Adv. Chem. Res. Vol. 56* **2019**, *86* (12), 117–152.

(6) Rosbottom, I.; Ma, C. Y.; Turner, T. D.; O'Connell, R. A.; Loughrey, J.; Sadiq, G.; Davey, R. J.; Roberts, K. J. Influence of Solvent Composition on the Crystal Morphology and Structure of P-Aminobenzoic Acid Crystallized from Mixed Ethanol and Nitromethane Solutions. *Cryst. Growth Des.* **2017**, *17* (8), 4151–4161. https://doi.org/10.1021/acs.cgd.7b00425.

(7) Perera, A.; Zoranić, L.; Sokolić, F.; Mazighi, R. A Comparative Molecular Dynamics Study of Water-Methanol and Acetone-Methanol Mixtures. *J. Mol. Liq.* **2011**, *159* (1), 52–59. https://doi.org/10.1016/j.molliq.2010.05.006.

(8) Marcus, Y. Preferential Solvation in Mixed Solvents X. Completely Miscible Aqueous Co-Solvent Binary Mixtures at 298.15 K. *Monatshefte fur Chemie* **2001**, *132* (11), 1387–1411. https://doi.org/10.1007/s007060170023.

(9) Bowron, D. T.; Soper, A. K.; Finney, J. L. Temperature Dependence of the Structure of a 0.06 Mole Fraction Tertiary Butanol-Water Solution. *J. Chem. Phys.* **2001**, *114* (14), 6203–6219. https://doi.org/10.1063/1.1354167.

(10) Falkowska, M.; Bowron, D. T.; Manyar, H. G.; Hardacre, C.; Youngs, T. G. A. Neutron Scattering of Aromatic and Aliphatic Liquids. *ChemPhysChem* **2016**, 2043–2055. https://doi.org/10.1002/cphc.201600149.

(11) Sillrén, P.; Swenson, J.; Mattsson, J.; Bowron, D.; Matic, A. The Temperature Dependent Structure of Liquid 1-Propanol as Studied by Neutron Diffraction and EPSR Simulations. *J. Chem. Phys.* **2013**, *138* (21). https://doi.org/10.1063/1.4807863.

(12) Soper, A. K. Computer Simulation as a Tool for the Interpretation of Total Scattering Data from Glasses and Liquids. *Mol. Simul.* **2012**, *38* (14–15), 1171–1185. https://doi.org/10.1080/08927022.2012.732222.

(13) Bowron, D. T.; Díaz Moreno, S. The Structure of a Concentrated Aqueous Solution of Tertiary Butanol: Water Pockets and Resulting Perturbations. *J. Chem. Phys.* **2002**, *117* (8), 3753–3762. https://doi.org/10.1063/1.1495397.

(14) Hardacre, C.; McMath, S. E. J.; Nieuwenhuyzen, M.; Bowron, D. T.; Soper, A. K. Liquid Structure of 1,3-Dimethylimidazolium Salts. *J. Phys. Condens. Matter* **2003**, *15* (1). https://doi.org/10.1088/0953-8984/15/1/320.

(15) Al-Madhagi, L. H.; Callear, S. K.; Schroeder, S. L. M. Hydrophilic and Hydrophobic Interactions in Concentrated Aqueous Imidazole Solutions: A Neutron Diffraction and Total X-Ray Scattering Study. *Phys. Chem. Chem. Phys.* **2020**, *22* (9), 5105–5113. https://doi.org/10.1039/c9cp05993h.

(16) Soper, A. K.; Barney, E. R. Extracting the Pair Distribution Function from White-Beam X-Ray Total Scattering Data. *J. Appl. Crystallogr.* **2011**, *44* (4), 714–726. https://doi.org/10.1107/S0021889811021455.

(17) Chater, P. A.; Keeble, D.; Wharmby, M.; Spain, T.; Filik, J.; Wilhelm, H. The Automated XPDF Beamline at Diamond Light Source. *Acta Crystallogr. Sect. A Found. Adv.* **2017**, *73* (a2), C69–C69. https://doi.org/10.1107/s2053273317095018.

(18) Zhou, Y.; Yamaguchi, T.; Ikeda, K.; Yoshida, K.; Otomo, T.; Fang, C.; Zhang, W.; Zhu, F. Dihydrogen Bonds in Aqueous NaBD4 Solution by Neutron and X-Ray Diffraction. *J. Phys. Chem. Lett.* **2020**, *11* (5), 1622–1628. https://doi.org/10.1021/acs.jpclett.9b03183.

(19) Song, S.; Peng, C. Viscosities of Binary and Ternary Mixtures of Water, Alcohol, Acetone, and Hexane. *J. Dispers. Sci. Technol.* **2008**, *29* (10), 1367–1372. https://doi.org/10.1080/01932690802313006.

(20) Benedetti, A. V.; Cilense, M.; Vollet, D. R.; Montone, R. C. Thermodynamic Properties of Liquid Mixtures. III. Acetone-Water. *Thermochim. Acta* **1983**, *66* (1–3), 219–223. https://doi.org/10.1016/0040-6031(93)85032-5.

(21) Toryanik, A. I.; Taranenko, V. N. Molecular Mobility and Structure in Water-Acetone Mixtures. *J. Struct. Chem.* **1988**, *28* (5), 714–719. https://doi.org/10.1007/BF00752054.

(22) Venables, D. S.; Schmuttenmaer, C. A. Spectroscopy and Dynamics of Mixtures of Water with Acetone, Acetonitrile, and Methanol. *J. Chem. Phys.* **2000**, *113* (24), 11222–11236. https://doi.org/10.1063/1.1328072.

(23) Idrissi, A.; Longelin, S.; Sokolić, F. Study of Aqueous Acetone Solution at Various Concentrations: Low-Frequency Raman and Molecular Dynamics Simulations. *J. Phys. Chem. B* **2001**, *105* (25), 6004–6009. https://doi.org/10.1021/jp004217r.

(24) Max, J. J.; Chapados, C. Infrared Spectroscopy of Acetone-Water Liquid Mixtures. I. Factor Analysis. *J. Chem. Phys.* **2003**, *119* (11), 5632–5643. https://doi.org/10.1063/1.1600438.

(25) Max, J. J.; Chapados, C. Infrared Spectroscopy of Acetone-Water Liquid Mixtures. Ii. Molecular Model. *J. Chem. Phys.* **2004**, *120* (14), 6625–6641. https://doi.org/10.1063/1.1649936.

(26) Kamogawa, K.; Kitagawa, T. Raman Difference Spectroscopy of the C-H Stretching Vibrations: Frequency Shifts and Excess Quantities for Acetone/Water and Acetonitrile/Water Solutions. *J. Phys. Chem.* **1986**, *90* (6), 1077–1081. https://doi.org/10.1021/j100278a024.

(27) Wu, N.; Li, X.; Liu, S.; Zhang, M.; Ouyang, S. Effect of Hydrogen Bonding on the Surface Tension Properties of Binary Mixture (Acetone-Water) by Raman Spectroscopy. *Appl. Sci.* **2019**, *9* (6). https://doi.org/10.3390/app9061235.

(28) McLain, S. E.; Soper, A. K.; Luzar, A. Orientational Correlations in Liquid Acetone and Dimethyl Sulfoxide: A Comparative Study. *J. Chem. Phys.* **2006**, *124* (7), 074502. https://doi.org/10.1063/1.2170077.

(29) McLain, S. E.; Soper, A. K.; Luzar, A. Investigations on the Structure of Dimethyl Sulfoxide and Acetone in Aqueous Solution. *J. Chem. Phys.* **2007**, *127* (17), 174515. https://doi.org/10.1063/1.2784555.

(30) Katayama, M.; Ozutsumi, K. The Number of Water-Water Hydrogen Bonds in Water-Tetrahydrofuran and Water-Acetone Binary Mixtures Determined by Means of X-Ray Scattering. *J. Solution Chem.* **2008**, *37* (6), 841–856. https://doi.org/10.1007/s10953-008-9276-0.

(31) Soper, A. K. Water: Two Liquids Divided by a Common Hydrogen Bond. *J. Phys. Chem. B* **2011**, *115* (48), 14014–14022. https://doi.org/10.1021/jp2031219.

(32) Shi, R.; Tanaka, H. Direct Evidence in the Scattering Function for the Coexistence of Two Types of Local Structures in Liquid Water. *J. Am. Chem. Soc.* **2020**, *142* (6), 2868–2875. https://doi.org/10.1021/jacs.9b11211.

(33) Fu, L.; Bienenstock, A.; Brennan, S. X-Ray Study of the Structure of Liquid Water. *J. Chem. Phys.* **2009**, *131* (23). https://doi.org/10.1063/1.3273874.

(34) Noda, K.; Ohashi, M.; Ishida, K. Viscosities and Densities at 298.15 K for Mixtures of Methanol, Acetone, and Water. *J. Chem. Eng. Data* **1982**, *27* (3), 326–328. https://doi.org/10.1021/je00029a028.

(35) Sun, H.; Wang, J. Solubility of Lovastatin in Acetone + Water Solvent Mixtures. *J. Chem. Eng. Data* **2008**, *53* (6), 1335–1337. https://doi.org/10.1021/je800063d.

(36) Long, B.; Xia, Y.; Deng, Z.; Ding, Y. Understanding the Enhanced Solubility of 1,3-Benzenedicarboxylic Acid in Polar Binary Solvents of (Acetone + Water) at Various Temperatures. *J. Chem. Thermodyn.* **2017**, *105* (October), 105–111. https://doi.org/10.1016/j.jct.2016.10.011.

(37) Sadeqzadeh, M.; Papaioannou, V.; Dufal, S.; Adjiman, C. S.; Jackson, G.; Galindo, A. The Development of Unlike Induced Association-Site Models to Study the Phase Behaviour of Aqueous Mixtures Comprising Acetone, Alkanes and Alkyl Carboxylic Acids with the SAFT-γ Mie Group Contribution Methodology. *Fluid Phase Equilib.* **2016**, *407*, 39–57. https://doi.org/10.1016/j.fluid.2015.07.047.

(38) Fetisov, E. O.; Mundy, C. J.; Schenter, G. K.; Benmore, C. J.; Fulton, J. L.; Kathmann, S. M. Nanometer-Scale Correlations in Aqueous Salt Solutions. *J. Phys. Chem. Lett.* **2020**, *11* (7), 2598–2604. https://doi.org/10.1021/acs.jpclett.0c00322.

(39) Hunter, C. A. Quantifying Intermolecular Interactions: Guidelines for the Molecular Recognition Toolbox. *Angew. Chemie - Int. Ed.* **2004**, *43* (40), 5310–5324. https://doi.org/10.1002/anie.200301739.